Field Trial of SDN-Controlled Probabilistic Constellation Shaping Supporting Multiple Rates Over a Coupled-Core Multi-Core Fiber

Field Trial of SDN-Controlled Probabilistic Constellation Shaping Supporting Multiple Rates Over a Coupled-Core Multi-Core Fiber

N. Sambo, A. Nespola, A. Sgambelluri, A. Marotta, *Member, IEEE*, L. Dallachiesa, *Member, IEEE*, R. Ryf, *Fellow, IEEE*, P. Castoldi, *Senior Member, IEEE*, A. Mecozzi, *Fellow, IEEE*, T. Hayashi, *Senior Member, IEEE*, A. Carena, *Senior Member, IEEE*, and C. Antonelli, *Senior Member, IEEE*

(Post-Deadline Paper)

***Abstract*—Space division multiplexing (SDM) is being investigated in support of traffic growth. SDM networks offer multiplexing over space and spectrum dimensions. Probabilistic constellation shaping (PCS) is a solution to optimize spectral efficiency by adapting the constellation of a M-ary quadrature amplitude modulated (QAM) signal to physical layer impairments. At the control plane, in the recent years NETCONF and YANG have been identified as the protocol and the data modeling language, respectively, for the configuration and management of network devices. Significant effort has also been directed to network disaggregation and vendor neutrality: an example is the work done within the OpenConfig consortium. In this article, we present a SDM field trial based on a deployed coupled-core four-core fiber, where a software-defined network (SDN) controller configures probabilistic constellation shaping through NETCONF, by optimizing spectral efficiency either with respect to the path length, or in response to degradations due to soft failures. The NETCONF protocol relies on the OpenConfig YANG data model to configure and manage transceivers. In the field trial the integrated data and control planes are demonstrated with multiple rates (800-850-900-950-1000 Gb/s) for optical reach values ranging from 910 km to 2730 km. Soft failures are also introduced and a characterization of their impact on transmission performance is provided in order to design the recovery strategy deployed by SDN controller. Indeed, depending on the changes in the electrical signal-to-noise ratio, the SDN controller reconfigures the constellation shaping to restore the optical connection affected by the failure with a reduced line rate.**

***Index Terms*—MCF, multi-core, NETCONF, probabilistic constellation shaping, SDM, SDN, YANG.**

I. Introduction

SPACE division multiplexing (SDM) based on parallel fibers, multi-core (MCFs), or multi-mode fibers (MMFs) is under investigation in support of traffic increase [1], and real-time transmission experiments have been recently reported [2], [3]. Multiple-input multiple-output (MIMO) coherent receivers are used to extract the signals transmitted in the fiber modes in the regime of strong coupling, as well as to compensate for linear propagation effects, such as chromatic dispersion, modal dispersion and mode-dependent loss [4], [5], [6]. Networks based on SDM can thus leverage multiplexing over two dimensions: space and frequency. In general, the usage of the spectrum can be optimized by adopting probabilistic constellation shaping (PCS) [7], [8], [9], which provides a fine trade-off between physical layer robustness (or more simply optical reach) and spectral efficiency by modifying the level of constellation shaping based on the specific path in a fiber-based network. However, PCS has been mainly studied and demonstrated for transmissions or networks over single-mode fibers, whereas much fewer investigations [10], [11] of its use in MCF- or MMF-based SDM systems have been reported, of which none using deployed fibers nor integration with software-defined network (SDN) control plane.

At the control-plane level, recently, relevant effort has been spent on disaggregation from software to the hardware and vendor neutrality [12], [13], [14], [15], with the involvement of vendors and operators within projects and consortia such as OpenConfig [16], OpenROADM [17], and the Telecom Infra Project (TIP) [18]. Several demonstrations have been completed and discussions are still ongoing to find agreements on data models providing unique descriptions of devices (e.g., terminal devices) as the basement for the implementation of the control plane, e.g., to configure transponders: central frequency, modulation format, etc. An output of the OpenConfig project is the

Manuscript received 5 December 2022; revised 2 March 2023; accepted 1 April 2023. Date of publication 6 April 2023; date of current version 27 June 2023. The previous version of this article was presented at the European Conference on Optical Communication. This work was supported in part by the Italian Government through Project PRIN2017 FIRST under Grant GA 2017HP5KH7 002 and in part by Project INCIPICT.

N. Sambo, A. Sgambelluri, and P. Castoldi are with the Scuola Superiore Sant'Anna, 56127 Pisa, Italy (e-mail: n.sambo@sssup.it; andrea.sgambelluri@santannapisa.it; castoldi@sssup.it).

A. Nespola is with the LINKS Foundation, 10138 Torino, Italy (e-mail: antonino.nespola@linksfoundation.com).

A. Marotta, A. Mecozzi, and C. Antonelli are with the Università Degli Studi Dell'Aquila, 67100 L'Aquila, Italy (e-mail: andrea.marotta@univaq.it; antonio.mecozzi@univaq.it; cristian.antonelli@univaq.it).

L. Dallachiesa and R. Ryf are with the Nokia Bell Labs, Murray Hill, NJ 07974-0636 USA (e-mail: lauren.dallachiesa@nokia-bell-labs.com; roland.ryf@nokia.com).

T. Hayashi is with the Sumitomo Electric Industries, Ltd., Yokohama 554-0024, Japan (e-mail: t-hayashi@sei.co.jp).

A. Carena is with the Politecnico di Torino, 10129 Torino, Italy (e-mail: andrea.carena@polito.it).

Color versions of one or more figures in this article are available at https://doi.org/10.1109/JLT.2023.3265277.

Digital Object Identifier 10.1109/JLT.2023.3265277

OpenConfig data model, which defines vendor-neutral configuration parameters (e.g., the central frequency) and encompasses vendor-specific solutions, which might be required to provide enhanced transmission performance. The NETCONF protocol [19], [20], [21] together with the YANG data modeling language [22] are identified as control plane solutions for the configuration and the management of network devices. In the context of SDM networks, NETCONF and YANG have been demonstrated for the control of MIMO-based transceivers in [21]. In [23], a YANG description of the physical topology of an SDM network is provided by extending the optical impairment-aware topology described by the Internet Engineering Task Force (IETF) [24]. However, NETCONF/YANG and their exploitation to control PCS transmission, especially in the context of SDM networks, still need to be deeply investigated.

In this paper, which is an extended version of [25], we present a field trial over the deployed SDM fiber infrastructure in the city of L'Aquila, Italy [26]. A SDN controller relies on the NETCONF protocol exploiting OpenConfig YANG data model [16] to configure constellation shaping in MIMO-based transceivers. Experimental results are reported both for normal operations (e.g., connection provisioning), and in the presence of soft failures (i.e., performance degradations). Performance is reported for a *spatial super-channel*, i.e., an optical connection exploiting a wavelength channel over all the four available cores; in particular, the four signals, one per core, are co-routed and jointly detected by the MIMO-based receiver. In the case of soft failures, we also present a soft failure management scheme based on electrical signal-to-noise ratio (eSNR) and generalized mutual information (GMI): a soft-failure is detected through eSNR measurements, which are then mapped into GMI in order to identify the most suitable shaping parameter in the presence of the experienced performance degradation. In this paper we supplement the results presented in [25] with additional details on the setup and on the deployed MCFs; we introduce the procedure deployed by the SDN controller to subscribe to "alarms" (depending on the measured eSNR), showing that a threshold on eSNR as the figure of merit can be set into the receiver agent to define the range of (unacceptable) quality of transmission (QoT); we also provide the back-to-back characterization, which is needed to design the recovery strategy at the SDN controller, i.e., to map eSNR and GMI, which will be used to decide the shaping parameter upon degradation. Measurements show that a set of dual-polarization probabilistically constellation shaped 32 quadrature amplitude modulation (PCS-32QAM) signals running at 30 Gbaud with different shaping levels enables aggregate net line rates per wavelength of 800, 850, 900, 950, and 1000 Gb/s in coupled-core four-core fiber over propagation distances of 2730 km, 2380 km, 1890 km, 1540 km, and 910 km, respectively. A soft failure is then emulated and the experiment shows that the reconfiguration of the PCS shaping level performed/implemented by the SDN controller permits to recover most of the traffic along the same path: 850 Gb/s out of the original 900 Gb/s.

II. State of the Art

Transmission over SDM systems, probabilistic constellation shaping, and SDN control plane have been investigated in the literature, especially individually. In particular, transmission experiments have been presented employing MIMO-based receivers to undo the coupling among spatial dimensions, as well as to compensate for chromatic dispersion, modal dispersion and mode-dependent loss, both over multi-mode [4], [5] and multi-core fibers [6]. In such works, we can refer to *spatial super-channels*, i.e., optical connections which are carried by the same wavelength channel (or portion of spectrum) over several spatial dimensions: e.g., all modes in MMFs or all cores in MCFs. In this case, all the signals transported by the cores or modes must be co-routed within the network and detected together by the MIMO receiver.

Probabilistic constellation shaping has been mainly investigated in the literature over single-mode fibers [7], [8]. Basically, fixing a constellation (e.g., 16QAM), symbols are transmitted with different probabilities aiming at limiting the transmission of symbols that are more subjects to errors. Such technique permits to enhance transmission robustness against physical layer impairments, at the expense of a spectral efficiency reduction. Differently, from a change of modulation format – e.g., from dual polarization 16QAM (DP-16QAM) to DP-8QAM that implies a spectral efficiency reduction by a 1.33 factor – PCS permits to obtain a better trade-off between robustness and spectral efficiency (e.g., from 5 bit/symbol to 4.79 bit/symbol, the spectral efficiency reduces by only 1.04). The performance of constellation shaping applied to QAM signals has been simulated in [7]. In [28], constellation shaping is successfully experimented applied to 64QAM and 32QAM signals, showing a mitigation of the non-linear phase noise. In [8], constellation shaping is tested over pure silica-core fiber and non-zero dispersion-shifted fiber. In [10] and [11], probabilistic constellation shaping is used in conjunction with MIMO in a 10-mode fiber and in a coupled-core 4-core fiber, respectively.

Regarding automation and control plane, to the best of our knowledge, there are no works designing and implementing an SDN control plane specifically for constellation shaping. In the context of SDN and NETCONF, a first YANG model addressing the control of SDM networks, also including MIMO detection, was presented in [21] in a testbed employing a 11 km six-mode 19-core fiber. Such model encompasses several attributes including the type of constellation (or modulation format) and the possibility to use MIMO. However, now, an alignment to the OpenConfig YANG model might be desired. Indeed, recently, activities in the OpenConfig consortium produced a common YANG model to control and manage transponders. Such model includes the Operational (OP) mode attribute to account for vendor-specific parameters such as forward error correction (FEC), and to include proprietary advanced transmission solutions; in particular, a specific OP mode value is mapped to specific transmission parameters (e.g., modulation format, coding, symbol rate). This mapping is a task of the agent at the transponder, which applies the configuration of the proper transmission parameters according to the OP mode value. Currently, the OpenConfig YANG model is not used for probabilistic constellation shaping neither for MIMO-based detection and, thus, related agents need to be designed.

Moreover, in general, probabilistic constellation shaping and NETCONF/YANG (including the OpenConfig model) and SDN

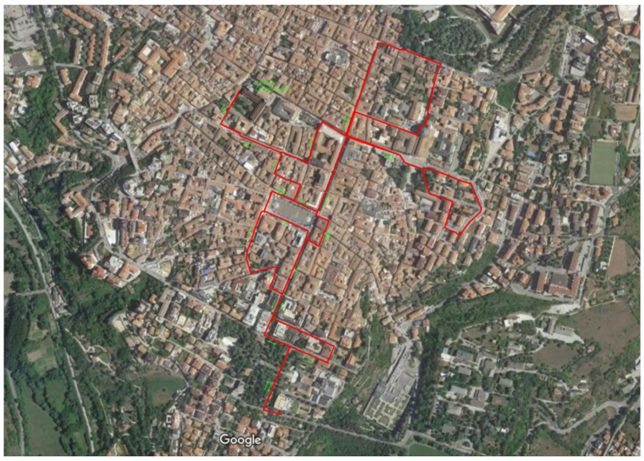

Fig. 1. Area in L'Aquila, Italy, where MCF is deployed.

have been mainly investigated in single-mode fibers. In contrast, their use in conjunction with coupled-core multi-core fibers is either unexplored or much less explored. A major implication of using coupled-core multi-core fibers is the need of MIMO-DSP techniques to extract the signals transmitted in the fiber cores, which couple strongly with each other in a random and frequency-dependent fashion during propagation – a channel characteristic that is absent in single-mode systems. This makes the successful implementation of an automated testbed including an SDN control plane configuring and managing probabilistic constellation shaping and MIMO receivers, an intrinsically challenging and relevant open problem. In this paper we address this problem by experimentally demonstrating an automated system employing probabilistic constellation shaping and MIMO on a field-deployed coupled-core MCF, controlled through NETCONF and YANG with the OpenConfig model.

III. Field Trial Set Up

The field trial was based on the coupled-core four-core fibers deployed in the city of L'Aquila, Italy, along the red path shown in Fig. 1 [27]. The main fiber parameters are summarized in Table I [26]. Fig. 2 shows the experimental setup, including data and control planes. The optical path was a four-fold recirculating loop consisting of 11 concatenated fiber strands forming a span of 69.3 km. For simplicity of illustration, the propagation distance will be expressed in multiples of 70 km throughout the next section.

A custom-built SDN controller holding a NETCONF plugin is responsible for transceiver configuration through the NETCONF protocol [19], [20], [21]. The OpenConfig (OC) model [6] – encompassing a set of vendor-neutral YANG data models – is adopted to configure transceivers at both transmitter (TX) and receiver (RX) sides. In particular, the OC terminal device model defines optical channel configuration parameters such as the central frequency and the output power. Moreover, within the OC model, OP modes have been introduced to also enable vendor-specific parameters such as FEC, and to include proprietary advanced transmission solutions. In this work, an OP mode

TABLE I
Parameters of the Deployed MCF

Fiber cross-section	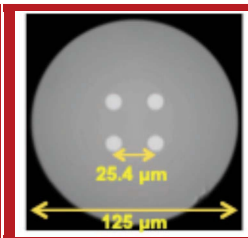
Fiber count in the cable	**12**
Features	Low-loss, cutoff shift
Suitable applications	Long-haul / point-to-point
MFD	10.1 µm at λ=1.55 µm (A_{eff} 80.9 µm^2)
Attenuation	0.170 to 0.175 dB/km at λ=1.55 µm
λ_{cc} (22-m)	1.41 to 1.51 µm
Transmission suitable band	C to L bands 1530 to 1625 nm

is associated to a specific probabilistic shaping level and all the OP modes used in this paper imply the adoption of MIMO at the receiver. Thus, we implemented two OpenConfig NETCONF agents (i.e., one at the TX side and one at RX side) using two docker containers to control the data plane devices.

Each agent is composed of two main components, as shown in Fig. 3: the NETCONF module (i.e., NETCONF server), implementing the control-plane interface towards the SDN controller, and the driver module, responsible for the interaction with the underlying data plane devices. The NETCONF module and the driver communicate with two custom-built sockets devoted to configuration and monitoring, *conf* and *mon* in Fig. 3, respectively. When an OpenConfig NETCONF agent receives on the NETCONF module a configuration message (e.g., the <edit-config> message), that includes a given OP mode, the driver module performs the mapping of the OP mode to the correct shaping level. The resulting configuration is then issued to the transmitter and to the MIMO receiver.

The OP mode values and shaping levels are reported in Table II together with their associated net rates *R* achievable per wavelength over the two polarizations and the four-cores of the coupled-core fiber.

Bit rates between 800 Gb/s and 1000 Gb/s can be set with 50 Gb/s granularity by adjusting the shaping parameter (S) of a 30 Gbaud PCS-32QAM signal working with a FEC overhead of 20%, and implemented with Maxwell-Boltzmann distributed symbols, the Constant Composition Distribution Matching (CCDM) algorithm [29], and the Probabilistic Amplitude Shaping (PAS) scheme [30]. Upon connection request, the SDN controller selects the most spectral efficient shaping supporting

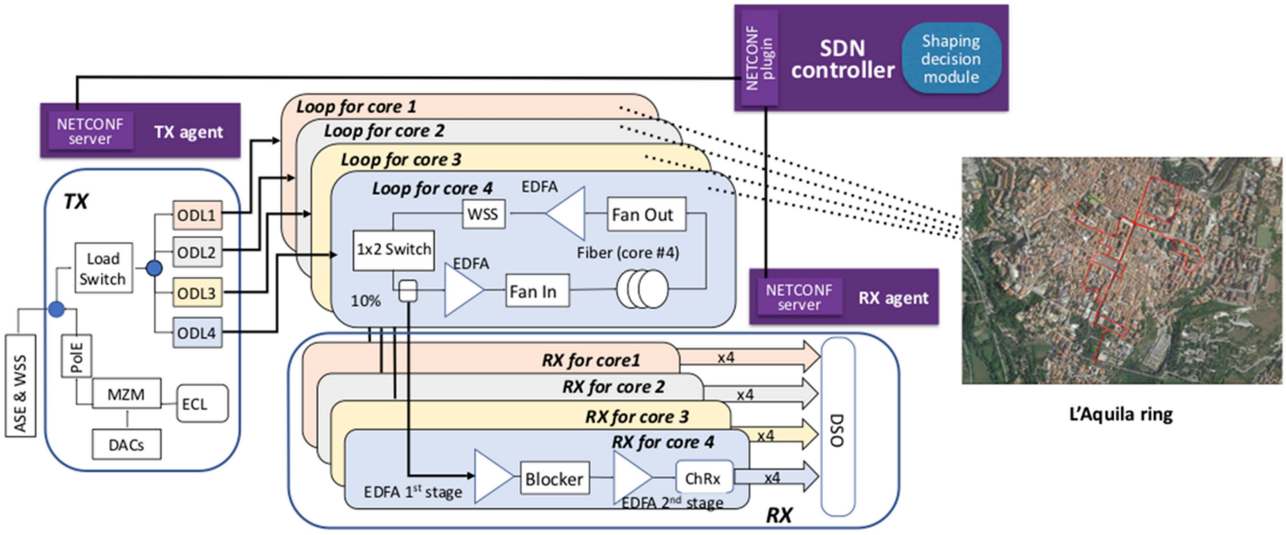

Fig. 2. Integrated data and control plane on field.

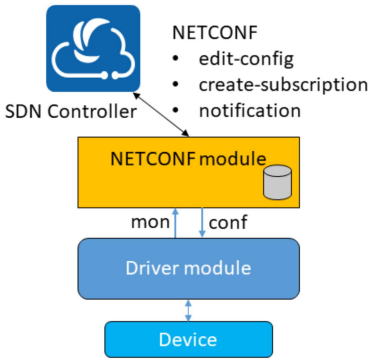

Fig. 3. NETCONF agent structure.

TABLE II
REFERENCE VALUES FOR OP MODE, SHAPING COEFFICIENT (S), RAW SPECTRAL EFFICIENCY (H), AND NET BIT-RATE (R)

OP mode	S (shaping)	H [bit/symb] [per core and polarization]	Overall net bit-rate R [Gb/s]
5	0.1132	4.17	800
4	0.0929	4.37	850
3	0.0724	4.58	900
2	0.0492	4.79	950
1	0	5	1000

the length of the computed path (*Shaping decision module* in Fig. 2). During provisioning the *Shaping decision module* consists of a lookup table based on the path length, which is designed through measurements, as explained in the next section. In the presence of soft failures, the *Shaping decision module* selects the shaping level according to the measured eSNR; more details will be provided in the next section. Then, the SDN controller sends a NETCONF <edit-config> message to both the TX and RX agents for TX and RX configuration. This message writes the transceiver configuration parameters values (e.g., central frequency, output power, and OP mode) selected by the SDN controller into the NETCONF server at each agent. Then, the agent interprets the configuration values, maps the OP mode to a specific shape, and configures the transceiver, loading the signal with the proper level of shaping into digital-to-analog converters (DACs), and, at the receiver, enabling also MIMO reception.

At the data plane, the loop also includes four wavelength selecting switches (WSS), configured as dynamic gain equalizing filters, and four two-stage single-mode amplifiers connected to the MCF fibre cores through fan-in and fan-out (FIFO) devices. A channel under test (CUT) in the centre of the WDM comb is generated using a <100 kHz External Cavity Laser (ECL), modulated at 30 GBaud with a single-polarization Mach-Zehnder Modulator (MZM) driven by two 60 GSa/s DACs. Polarization multiplexing is emulated by splitting the optical signal and recombining two delayed replicas in orthogonal polarizations (PolE). To mimic WDM transmission, further 20 channels (10 on each side with respect to the CUT), 50 GHz spaced, are emulated by shaping ASE noise using a high-resolution WSS (ASE & WSS). The number of WDM channels was limited by the total transmit-power constraints imposed by the FIFO devices.

The aggregated WDM signal is then split into four paths (one per core) and decorrelated with optical delay lines (ODL) with a relative delay of ∼100 ns. The resulting signals are injected in the recirculating loop through solid-states 1x2 switches, while an additional load switch is used to improve the extinction ratio of the signals. At the receiver, for each core the propagated WDM signal is extracted from the loop, filtered (Blocker in the schematic) between the two stages of an optical amplifier and detected by a polarization-diverse coherent receiver (ChRx). The resulting 16 electrical signals are captured by a digital storage

oscilloscope (DSO) operating at 80 GSa/s. Finally, the digitized signals are down-sampled to 2 samples per symbol and processed offline. After chromatic dispersion and frequency-offset compensation, an 8x8 MIMO processing based on frequency domain equalizers allows to demultiplex each of the 8 tributaries (given by the four space dimensions, each including two polarization modes).

IV. Experimental Results

In this section we first show connection-provisioning experiments and then we validate a recovery strategy against soft failures. We use GMI as a figure of merit for QoT, based on the assumption that a system of the kind considered here can operate with modern optical coherent receivers that combine complex multi-level modulation with binary soft-decision forward error correction (SD-FEC) in the framework of the bit-interleaved coded modulation (BICM) scheme. Accordingly, we assumed to perform constellation demapping and binary FEC decoding in two separate steps, and we estimated the GMI under the AWGN assumption using digital signal processed symbols (after filtering, sampling, synchronization, and equalization) and the Montecarlo approximation [31]

$$GMI = H - G$$

$$G = \frac{1}{N}\sum_{n=1}^{N}\sum_{k=1}^{log_2(M)} \log_2 \frac{\sum_{x_m \in \mathcal{X}} exp\left(-\frac{|y_n - x_m|^2}{\sigma^2}\right) P_{x_m}}{\sum_{x_m \in \mathcal{X}(k,b_{n,k})} exp\left(-\frac{|y_n - x_m|^2}{\sigma^2}\right) P_{x_m}}, \tag{1}$$

where H is the entropy of a PCS *M-QAM* constellation, G represents the loss of information due to propagation, x_m is the *m-th* symbol in the constellation alphabet transmitted with probability P_{x_m}, σ^2 is the noise variance, y_n is the *n-th* received symbol (out of a total of N symbols), $b_{n,k}$ is the *k-th* bit of the *n-th* transmitted symbol and $\mathcal{X}(k,b)$ is a subset of the constellation alphabet, $\mathcal{X}$, which contains bit $b \in [0,1]$ in the *k-th* bit position.

To provide a fair comparison between OP modes and to define a threshold for acceptable QoT, the normalized GMI (NGMI) was introduced [28] as it provides a figure of merit independent of the level of shaping. This is defined as

$$NGMI = 1 - \frac{H - GMI}{\log_2(M)} \tag{2}$$

and in [28] it was shown that considering an ideal FEC implementation with 20% overhead, an NGMI threshold ($NGMI_{th}$) equal to 0.83 is sufficient to ensure error-free transmission. However, in this work we set $NGMI_{th}$ at 0.94, to account for the actual FEC performance loss and practical implementation constraints. Note that this value is conservatively slightly higher than the typical value of 0.9, which guarantees post-FEC error-free transmission for most realistic SD-FEC algorithms [28] with 20% overhead.

A. Connection Provisioning

To optimize connection provisioning, a comprehensive experimental characterization of the system performance has been carried out. We measured GMI for all operational modes sweeping both distance and optical power over a wide range of values. Fig. 4 partially reports these measurements by showing the achieved GMIs (per core and polarization) having fixed the launched power at the optimal value of 0 dBm per channel. Note that maximum GMIs in back-to-back, are slightly lower with respect to the theoretical maximum values (H of Table II) because of non-ideal TX and RX components. For every OP modes listed in Table II, we extracted the GMI thresholds (GMI_{th}) corresponding to $NGMI_{th} = 0.94$. Then, GMI thresholds drive the maximum propagation distances L_{max} for each shaping level: all values are reported in the Table III.

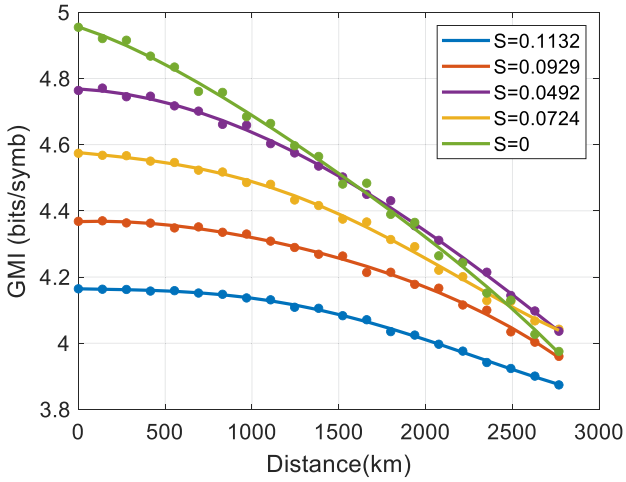

Fig. 4. GMI vs. distance at optimal power (0 dBm).

TABLE III
Values of GMI_{TH} and Optical Reach (L_{MAX})

OP mode	S	GMI_{th}	L_{max} [km]
5	0.1132	3.87	2730
4	0.0929	4.07	2380
3	0.0724	4.28	1890
2	0.0492	4.49	1540
1	0	4.7	910

Information related to shaping values, OP modes, and optical reaches were then loaded in the SDN controller to drive the *Shaping decision module* of the SDN controller.

At this point a connection provisioning experiment was performed. A request for a connection over a 1800-km path is sent to the SDN controller: based on the data stored (reported in Table III), the *Shaping decision module* at the SDN controller selected the OP mode number 3 with a shaping S = 0.0724. Thus, the SDN controller sent the <edit-config> message to the TX and RX agents. Fig. 5 shows the content of the control plane message: a central frequency of 193.9 THz and 0 dBm launch power were configured; OP mode 3 was set. Each agent mapped the given OP mode to the correct shaping profile (see Table III) to be loaded. The selected OP mode supported 900 Gb/s (Table II)

```
<components xmlns="http://openconfig.net/yang/platform">
  <component>
    <name>channel-1</name>
    <optical-channel xmlns="http://openconfig.net/yang/terminal-device">
      <config>
        <frequency>193900000</frequency>
        <target-output-power>0</target-output-power>
        <operational-mode>3</operational-mode>
      </config>
    </optical-channel>
  </component>
</components>
```

Fig. 5. <edit-config> message received by the TX agent.

along the 4 cores and admits a maximum optical reach of 1890 km.

B. Reliability Against Soft Failures

A desired functionality for future autonomous optical networks is the capability to adapt the transmission to physical layer changes, e.g., to recover the connection (or part of it) after a soft failure.

To do that, we leverage QoT monitoring at receiver side and transceiver back-to-back characterization to implement an approach to recover as much capacity as possible.

To detect QoT degradation we must monitor GMI as every operational modes has a minimum required threshold to guarantee the service. An efficient approach to evaluate GMI in real-time is to infer it from the evaluation of the eSNR, i.e., the electrical signal-to-noise ratio measured over the received samples. eSNR can be computed from the statistics of received and equalized symbols as:

$$\sigma^2 = \frac{1}{\log_2(M)} \sum_m \sigma_m^2$$

$$eSNR = \frac{\sum_m P_{x_m} |x_m|^2}{\sigma^2} \tag{3}$$

where σ_m^2 is the noise variances impinging the *m-th* symbol in the alphabet. To determine the actual relationship between GMI and eSNR, dependent on TX and RX implementations, we carried out a comprehensive back-to-back characterization. Using a noise loading technique to adjust the OSNR level, we were able to change the working condition of the transceiver by sweeping the GMI and eSNR over a broad range of values: results are reported in Fig. 6 for all different OP modes.

This characterization allows to define the relationship between GMI and eSNR and we can use it to determine the recovery strategy if QoT degradation is detected. If from one side we are sure the eSNR fully captures potential penalties deriving from actual transceiver implementation, we must validate if it is valid also for signals impacted by the non-linear propagation in the coupled-core multi-core fiber. In fact, even at the optimal launch power a non-negligible amount of non-linear interference is impinging the signal.

We experimentally validated this condition by propagating along a path of 1400 km. To see GMI and eSNR variations, also in this case we applied the noise loading technique at transmitter:

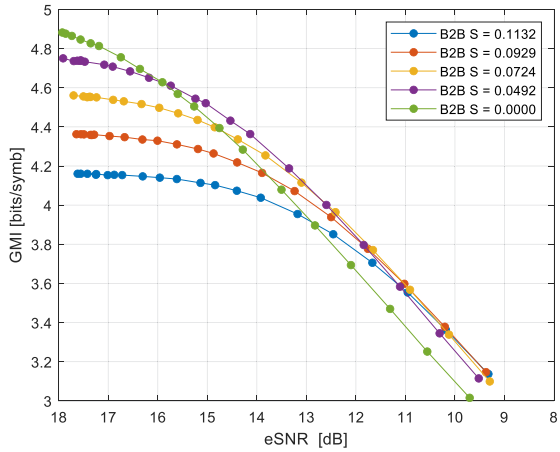

Fig. 6. GMI vs. eSNR: Measurements in back-to-back conditions capturing transceiver actual implementation.

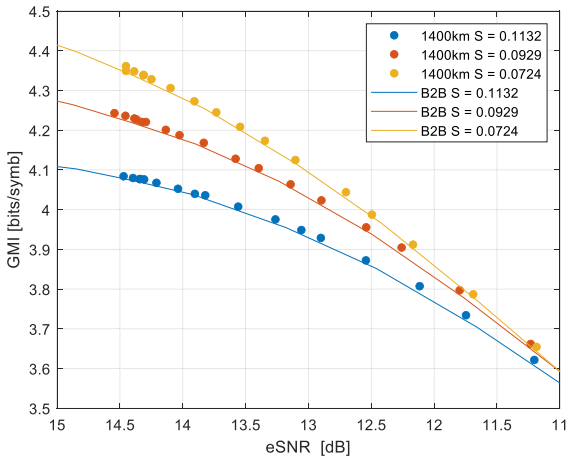

Fig. 7. GMI vs. eSNR: Measurements after a propagation on a path of 1400 km (dots) compared to back-to-back data (solid lines).

the actual OSNR accumulated along the transmission link can be reduced.

The perfect overlap between of the back-to-back curves (reported as solid lines in Fig. 7) and the measurement after the propagation is a proof that the back-to-back characterization is valid at any distance. This result implies that any transceiver (or at least one per class) can be characterized once during

```
<?xml version="1.0" encoding="UTF-8"?>
<rpc xmlns="urn:ietf:params:xml:ns:netconf:base:1.0" message-id="1">
 <create-subscription xmlns="urn:ietf:params:xml:ns:netconf:notification:1.0">
  <stream>openconfig</stream>
  <filter type="xpath" octd="http://openconfig.net/yang/terminal-device" select="/octd:esnr-change[octd:esnr<=14]"/>
 </create-subscription>
</rpc>
```

Fig. 8. <create-subscription> message sent to the RX agent.

```
<?xml version="1.0" encoding="UTF-8"?>
<notification xmlns="urn:ietf:params:xml:ns:netconf:notification:1.0">
  <eventTime>2022-09-05T08:51:32.517635+00:00</eventTime>
  <failure xmlns=http://openconfig.net/yang/terminal-device>
    <port>channel-1</port>
    <reason>esnr</reason>
    <level>14.0</level>
  </failure>
</notification>
```

Fig. 9. <notification> message sent by the RX agent.

manufacturing process and its GMI vs. eSNR relationship is the set of data needed by the SDN controller to operate, without any further in-field refinement process. The GMI vs. eSNR relationship must be stored in the *Shaping decision module* to allow the application of the shaping reconfiguration we propose in the following. In particular, a soft failure is detected based on measured eSNR, which is reported to the SDN controller through an "alarm", then, the Shaping decision module maps the eSNR to the GMI, which is finally used to identify the most suitable shaping level for reconfiguration.

Then, we conducted an experiment to demonstrate the five steps of the recovery process: 1) definition of QoT threshold to generate alarm (through <create-subscription> message), 2) detection of a QoT degradation, 3) alarm generation (through <notification> message), 4) shaping decision, and 5) shaping reconfiguration.

We started with an active connection with OP mode 3 (S = 0.0724) running over a path with a length of 1400 km. In normal conditions the receiver detects eSNR = 14.5 dB corresponding to GMI = 4.35. This value is above the required GMI threshold of 4.28, so the connection is in service.

Thanks to the characterization, the SDN controller identified that an eSNR of 14 dB would be associated to an unacceptable QoT ($\mathrm{GMI_{th}} = 4.28$). Thus, such an eSNR value measured at the receiver should generate an alarm. To inform the RX agent about this value, the SDN controller sent a <create-subscription> message to the RX agent: such message automatically subscribes the SDN controller to events described with the message. In particular, Fig. 8 shows the content of the <create-subscription> message reporting the threshold to the eSNR, which should generate a notification (or alarm) when the monitored eSNR falls below or is equal to that threshold of 14 dB.

Then we mimic a soft failure by degrading the OSNR: we used the same noise loading approach used in the characterization phase inserting some extra optical noise in front of the receiver. When the eSNR surpassed the critical value of 14 dB, the RX agent sent to the SDN controller a <notification> message (shown in Fig. 9) implementing the alarm and reporting the measured eSNR. The SDN controller, based on the b2b characterization, re-configures the connection to the OP mode 4 (S = 0.0929): it has a predicted GMI equal to 4.17 that is above the associated $\mathrm{GMI_{th}} = 4.07$. The lapse of time between failure detection and the start of reconfiguration is around 225 ms, measured from the time the agent at the receiver sends the <notification> message to the SDN controller to the time both the agents at the transmitter and receiver receive the <edit-config> message imposing the new configuration. The reconfiguration time at the data plane is not reported because of the lack of a real-time receiver, required to reveal when the transmission is stable after reconfiguration. Note that, when reconfiguring the shaping level, transmission is interrupted, as it would occur in the case of modulation format change (e.g., from DP-16QAM to DP-QPSK). The proposed reconfiguration permits to recover 850 Gb/s out of the original 900 Gb/s along the same path.

V. Conclusion

We have presented the first field trial of a SDN-controlled PCS transmission over SDM based on a deployed coupled-core four-core fiber. Shaping values enable distance adaptation and multiple rates of 800, 850, 900, 950, and 1000 Gb/s per wavelength. Based on characterization performed on the deployed transmission system, the SDN controller optimizes connection capacity by selecting the shaping according to the required optical reach. Dynamic shaping reconfiguration allows also to recover traffic upon soft failure: in particular, an SDN-controlled shaping adaptation strategy based on back-to-back transceiver characterization is demonstrated.

References

[1] P. J. Winzer, "Scaling optical fiber networks: Challenges and solutions," *Opt. Photon. News*, vol. 26, no. 3, pp. 28–35, Mar. 2015.

[2] M. Mazur et al., "Real-time transmission over 2x55 km all 7-core coupled-core multi-core fiber link," in *Proc. Opt. Fiber Commun. Conf.*, 2022, pp. 1–3, Paper Th4A.1.

[3] M. Mazur et al., "Real-time MIMO transmission over field-deployed coupled-core multi-core fibers," in *Proc. Opt. Fiber Commun. Conf.*, 2022, pp. 1–3, Paper Th4B.8.
[4] S. Randel et al., "6×56- Gb/s mode-division multiplexed transmission over 33-km few-mode fiber enabled by 6×6 MIMO equalization," *Opt. Exp.*, vol. 19, no. 17, pp. 16697–16707, Aug. 2011.
[5] R. Ryf et al., "Mode-division multiplexing over 96 km of few-mode fiber using coherent 6×6 MIMO processing," *J. Lightw. Technol.*, vol. 30, no. 4, pp. 521–531, Feb. 2012.
[6] R. Ryf et al., "Transmission over randomly-coupled 4-core fiber in field-deployed multi-core fiber cable," in *Proc. Eur. Conf. Opt. Commun.*, 2020, pp. 1–4, doi: 10.1109/ECOC48923.2020.9333277.
[7] M. P. Yankov, D. Zibar, K. J. Larsen, L. P. B. Christensen, and S. Forchhammer, "Constellation shaping for fiber-optic channels with QAM and high spectral efficiency," *IEEE Photon. Technol. Lett.*, vol. 26, no. 23, pp. 2407–2410, Dec. 2014.
[8] F. P. Guiomar et al., "Comparing different options for flexible networking: Probabilistic shaping vs. hybrid subcarrier modulation," in *Proc. IEEE Eur. Conf. Opt. Commun.*, 2017, pp. 1–3, doi: 10.1109/ECOC.2017.8346048.
[9] D. Pilori et al., "Comparison of probabilistically shaped 64QAM with lower cardinality uniform constellations in long-haul optical systems," *J. Lightw. Technol.*, vol. 36, no. 2, pp. 501–509, Jan. 2018.
[10] S. Beppu et al., "402.7-Tb/s MDM-WDM transmission over weakly coupled 10-mode fiber using rate-adaptive PS-16QAM signals," *J. Lightw. Technol.*, vol. 38, no. 10, pp. 2835–2841, May 2020.
[11] D. Soma et al., "50.47-Tbit/s standard cladding ultra-low-loss coupled 4-core fiber transmission over 9,150 km," in *Proc. Opt. Fiber Commun. Conf. Exhib.*, 2021, pp. 1–3.
[12] E. Riccardi, P. Gunning, G. de Dios, M. Quagliotti, V. Lopez, and A. Lord, "An operator view on the introduction of white boxes intooptical networks," *J. Lightw. Technol.*, vol. 36, no. 15, pp. 3062–3072, Aug. 2018.
[13] N. Sambo et al., "Experimental demonstration of a fully disaggregated and automated white box comprised of different types of transponders and monitors," *J. Lightw. Technol.*, vol. 37, no. 3, pp. 824–830, Feb. 2019.
[14] D. Scano, A. Giorgetti, S. Fichera, A. Sgambelluri, and F. Cugini, "Operational mode and slicing adaptation in OpenConfig disaggregated optical networks," in *Proc. Opt. Fiber Commun. Conf. Exhib.*, 2020, pp. 1–3.
[15] L. Nadal et al., "Programmable disaggregated multi-dimensional S-BVT as an enabler for high capacity optical metro networks," *J. Opt. Commun. Netw.*, vol. 13, no. 6, pp. C31–C40, Jun. 2021.
[16] [Online]. Available: https://www.openconfig.net/
[17] [Online]. Available: http://www.openroadm.org
[18] [Online]. Available: https://telecominfraproject.com/
[19] R. Enns, M. Bjorklund, J. Schoenwaelder, and A. Bierman, "Network configuration protocol (NETCONF)," Jun. 2011.
[20] M. Dallaglio, N. Sambo, F. Cugini, and P. Castoldi, "Control and management of transponders with NETCONF and YANG," *J. Opt. Commun. Netw.*, vol. 9, no. 3, pp. B43–B52, Mar. 2017.
[21] R. Muñoz et al., "SDN control of sliceable multidimensional (spectral and spatial) transceivers with YANG/NETCONF," *J. Opt. Commun. Netw.*, vol. 11, no. 2, pp. A123–A133, Feb. 2019, doi: 10.1364/JOCN.11.00A123.
[22] M. Bjorklund, "YANG – A data modeling language for the network configuration protocol (NETCONF)."
[23] S. Fichera, N. Sambo, C. Antonelli, A. Mecozzi, and P. Castoldi, "Physical topology abstraction for SDM optical networks," in *Proc. Opt. Netw. Des. Modelling*, 2020, pp. 1–5.
[24] Y. Lee et al., "A YANG data model for optical impairment-aware topology," 2022.
[25] N. Sambo et al., "Field trial of SDN-controlled probabilistic constellation shaping supporting multiple rates over a coupled-core multi-core fiber," in *Proc. Eur. Conf. Opt. Commun.*, 2022, pp. 1–4.
[26] T. Hayashi et al., "Field-deployed multi-core fiber testbed," in *Proc. IEEE 24th Optoelectron. Commun. Conf., Int. Conf. Photon. Switching Comput.*, 2019, pp. 1–3, doi: 10.23919/PS.2019.8818058.
[27] C. Antonelli et al., "The City of L'Aquila as a living lab: The INCIPICT project and the 5G trial," in *Proc. IEEE 5G World Forum*, 2018, pp. 410–415.
[28] D. Pilori, A. Nespola, F. Forghieri, and G. Bosco, "Non-linear phase noise mitigation over systems using constellation shaping," *J. Lightw. Technol.*, vol. 37, no. 14, pp. 3475–3482, Jul. 2019.
[29] P. Schulte and G. Böcherer, "Constant composition distribution matching," *IEEE Trans. Inf. Theory*, vol. 62, no. 1, pp. 430–434, Jan. 2016.
[30] G. Bocherer, F. Steiner, and P. Schulte, "Bandwidth efficient and rate-matched low-density parity-check coded modulation," *IEEE Trans. Commun.*, vol. 63, no. 12, pp. 4651–4665, Dec. 2015.
[31] A. Alvarado, T. Fehenberger, B. Chen, and F. M. J. Willems, "Achievable information rates for fiber optics: Applications and computations," *J. Lightw. Technol.*, vol. 36, no. 2, pp. 424–439, Jan. 2018.